



# Robust fixed-time attitude stabilization control of flexible spacecraft with actuator uncertainty

Lu Cao · Bing Xiao · Mehdi Golestani

Received: 13 August 2019 / Accepted: 23 March 2020 / Published online: 22 April 2020  
© Springer Nature B.V. 2020

**Abstract** A robust fixed-time control framework is presented to stabilize flexible spacecraft's attitude system with external disturbance, uncertain parameters of inertia, and actuator uncertainty. As a stepping stone, a nonlinear system having faster fixed-time convergence property is preliminarily proposed by introducing a time-varying gain into the conventional fixed-time stability method. This gain improves the convergence rate. Then, a fixed-time observer is proposed to estimate the uncertain torque induced by disturbance, uncertain parameters of inertia, and actuator uncertainty. Fixed-time stability is ensured for the estimation error. Using this estimated knowledge and the full-states' measurements, a nonsingular terminal sliding controller is finally synthesized. This is achieved via a nonsingular and faster terminal sliding surface with faster convergence rate. The closed-loop attitude stabilization system is proved to be fixed-time stable with the convergence time independent of initial states. The

attitude stabilization performance is robust to disturbance and uncertainties in inertia and actuators. Simulation results are also shown to validate the attitude stabilization performance of this control approach.

**Keywords** Flexible spacecraft · Fixed-time stability · Attitude stabilization · Actuator uncertainty · Uncertain inertia · Robust control

## 1 Introduction

### 1.1 Motivation

Although many attitude controllers have been developed for flexible spacecraft with large flexible communication antenna and solar paddle [1, 2], most of them stabilized the states of the attitude system as the time approaches infinity. Many missions demand fast attitude maneuvering [3]. To meet this requirement, the finite-time stability (FTS) concept is available. It provides system states with finite-time convergence. However, this finite-time convergence depends on initial states [4]. A prior precise estimation of the settling time cannot be obtained. Unlike the FTS [5], the fixed-time stability [6] is efficient to guarantee a desired finite convergence time despite any initial states. Only the control gains determine the settling time. The system states' convergence rate can be predefined off-line [7]. However, the converging rate ensured by the current fixed-time controllers is not fast enough.

---

L. Cao  
National Innovation Institute of Defense Technology,  
Chinese Academy of Military Sciences, Beijing 100071,  
China  
e-mail: caolu\_space2015@163.com

B. Xiao (✉)  
School of Automation, Northwestern Polytechnical  
University, Xi'an 710072, China  
e-mail: bxiaobing@gmail.com

M. Golestani  
Young Researchers and Elite Club, Qazvin Branch,  
Islamic Azad University, Qazvin, Iran  
e-mail: m.golestani@qiau.ac.ir

The current fixed-time attitude controllers for flexible spacecraft are developed by assuming that all actuators do not have any uncertainty, i.e., there is no error between actuator's commanded input and its actual output. This assumption may be not met. Actuator uncertainty may exist in practice, and should be addressed during attitude controller design. Otherwise, attitude control performance may be deteriorated and even mission failure may be resulted [8]. However, this problem is still open.

To achieve high-accuracy attitude control for spacecraft, external disturbance and uncertain inertia should be accommodated further. For adaptive control-based disturbance rejection approaches, the bound of disturbance and uncertain inertia is estimated and then compensated [9]. This approach lets their controllers have certain conservativeness. To avoid this drawback, the observer-based control schemes are widely seen [10]. However, most of the observer-based controls ensure zero estimation error after infinity time [11]. Besides the estimation rate, a critical disadvantage of the existing observers is that the disturbance's bound should be known or the disturbance's time derivative should be zero [12]. The issue of relaxing such constraints should be addressed.

## 1.2 Literature review

Recent years have witnessed a lot of attention to the flexible spacecraft attitude control problem. Many control schemes have been presented, including the backstepping control [13], the proportional-derivative control [14], the  $\mathcal{H}_\infty$  control [15], the adaptive control [16], the passivity-based control [17], the active disturbance rejection [18], the disturbance observer-based control [19], and so forth [20,21]. To meet the vital requirements including fast convergence rate and high pointing accuracy, attitude control design via the sliding mode control theory (SMC) has got significant consideration [22]. Aiming to control the attitude within a prescribed time, the terminal SMC (TSMC) was utilized in [23]. However, the TSMC suffers from singularity. To avoid this problem, many non-singular attitude TSMC (NTSMC) approaches have been reported [24]. In practice, actuator uncertainty may exist due to aging or malfunction of actuator's components. Considering this issue and applying the nonsingular TSMC [25], the fast TSMC [26], the backstepping control [27],

and the integral backstepping [28], many attitude stabilization controllers are seen to achieve finite-time convergence.

Although the finite-time controllers for spacecraft attitude system have certain advantages, the precise estimation of the settling time cannot be obtained. To solve this challenge, two relative position and attitude stabilization controllers with fixed-time convergence were presented to achieve the fly-around maneuver for a non-cooperative target [29,30]. A fixed-time control law was presented in [31] with the attitude tracking errors stabilized after fixed time despite uncertainties. In [32], the fixed-time attitude tracking issue without singularity was investigated. The predefined settling time of the tracking errors was achieved, but a sluggish response was seen when system states were near the origin.

To achieve high-pointing attitude control with disturbance rejected, one way would be to use observer-based controller [33]. Considering disturbance as an unknown input, employing the unknown input observer (UIO) [34] to estimate disturbances has received more and more attention. The development of UIO-based attitude controller for spacecraft was discussed in [35]. By a combination of Lyapunov function and extended-state observer, an attitude controller was presented in [36] with actuator saturation constraint solved. Using an adaptive extended-state observer, another attitude controller having capability of handling actuator uncertainty and achieving robustness as well as precise tracking accuracy was proposed in [37]. By estimating the unmeasurable modal variables, a distributed adaptive attitude controller has been reported in [38].

## 1.3 Contributions

Motivated by solving above three challenges, this paper presents an observer-based robust control approach for flexible spacecraft's attitude stabilization maneuvers with fixed convergence time. The main features of this study are highlighted as follows.

- (1) The conventional fixed-time stability theorem [39] is extended in this paper to decrease the settling time. A new stable system, based on which the main result of the paper is presented, is developed with its settling time shorter than [39].
- (2) Inspired by [33], a fixed-time nonlinear observer to reconstruct the lumped uncertainties is devel-

oped. Any prior knowledge of the total uncertainties is not required. Unlike the existing disturbance observers [12], the restrictions on the uncertainties is relaxed. Moreover, another feature of this observer is that the estimation error is finite-time stable regardless of initial estimation errors.

- (3) By designing a novel fixed-time terminal sliding surface, a robust attitude control law is proposed for flexible spacecraft with external disturbance, uncertainties in inertia parameters, and actuators accommodated.

### 1.4 Paper organization

The rest of this paper is organized as follows. Section 2 introduces the attitude system model of a flexible spacecraft and formulates its attitude control problem. Section 3 presents an estimation-based control framework to ensure superior attitude stabilization performance after a fixed time. Simulation results are shown in Sect. 4 followed by conclusion in Sect. 5 to end the paper.

## 2 System model and problem formulation

Let  $\mathcal{R}$  (respectively,  $\mathcal{R}_+$ ) denote the set of real (respectively, positive real) numbers.  $\mathcal{R}^{m \times n}$  represents the set of  $m$  by  $n$  real matrices.  $A^T$  is the transpose of a matrix  $A \in \mathcal{R}^{m \times n}$ , and  $A^{-1}$  is its left inverse if  $A$  has full column rank.  $\|\cdot\|$  denotes the vector or matrix's Euclidean norm.  $I_n$  is the identity matrix of  $n \times n$ .  $\mathbf{0}$  is a zero vector or matrix with appropriate dimension. For any scalar  $\gamma \in \mathcal{R}$  and any vector  $z = [z_1, z_2, z_3]^T \in \mathcal{R}^3$ ,

one defines  $z^\times = \begin{bmatrix} 0 & -z_3 & z_2 \\ z_3 & 0 & -z_1 \\ -z_2 & z_1 & 0 \end{bmatrix}$  and  $\text{sig}(z)^\gamma =$

$[|z_1|^\gamma \text{sgn}(z_1), |z_2|^\gamma \text{sgn}(z_2), |z_3|^\gamma \text{sgn}(z_3)]^T$ , where  $\text{sgn}(\cdot)$  is the sign function. For any vector  $v = [v_1, v_2, \dots, v_n]^T \in \mathcal{R}^n$ ,  $\text{diag}(v) \in \mathcal{R}^{n \times n}$  represents a

diagonal matrix given by  $\text{diag}(v) = \begin{bmatrix} v_1 & 0 & \dots & 0 \\ 0 & v_2 & \dots & 0 \\ \vdots & \vdots & \ddots & \vdots \\ 0 & 0 & \dots & v_n \end{bmatrix}$ .

$\exp(\cdot)$  denotes the exponential function.

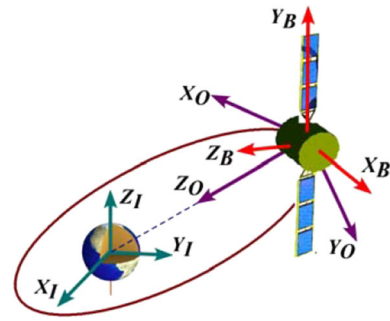


Fig. 1 The coordinate reference frame system

### 2.1 Modeling of flexible spacecraft attitude system

Three coordinate reference frames are usually involved when establishing spacecraft's attitude control system, as shown in Fig. 1. There are the inertial frame  $\mathcal{F}_I$ , the orbit reference frame  $\mathcal{F}_O$ , and the body-fixed frame  $\mathcal{F}_B$ . In this work,  $\mathcal{F}_I$  is chosen to be the Earth-Centered Inertial frame  $\mathcal{F}_I(X_I, Y_I, Z_I)$  with its origin at the center of the Earth.  $\mathcal{F}_O(X_O, Y_O, Z_O)$  rotating about the  $Y_O$  axis with respect to the frame  $\mathcal{F}_I$  at the orbital rate  $\omega_0 \in \mathcal{R}_+$ , has its origin located in the mass center of the satellite. The axis of that reference frame are chosen such that the roll axis  $X_O$  is in the flight direction, the pitch axis  $Y_O$  is perpendicular to the orbital plane, and the yaw axis  $Z_O$  points toward the center of the Earth. The frame  $\mathcal{F}_B(X_B, Y_B, Z_B)$  has the same origin as the orbit frame, and its axes fixed in the spacecraft's body and coincide with the principal axis of inertia.

Let  $\theta = [\theta, \phi, \psi]^T \in \mathcal{R}^3$  denote the attitude Euler angles of the spacecraft with respect to  $\mathcal{F}_O$ .  $\omega \in \mathcal{R}^3$  is the inertial angular velocity vector with respect to  $\mathcal{F}_I$  and expressed in  $\mathcal{F}_B$ .  $J \in \mathcal{R}^{3 \times 3}$  is the spacecraft's inertia expressed in the  $\mathcal{F}_B$ , i.e.,  $J = J_0 + \Delta J$ , where  $J_0 \in \mathcal{R}^{3 \times 3}$  and  $\Delta J \in \mathcal{R}^{3 \times 3}$  represents the nominal and the uncertain inertia, respectively. Then, for a flexible spacecraft, its attitude system can be modeled as [40].

$$\omega = R(\theta) \dot{\theta} - \omega_c(\theta) \tag{1}$$

$$J \dot{\omega} + \omega^\times (J \omega + \delta^T \dot{\chi}) + \delta^T \ddot{\chi} = \tau + \tau_d \tag{2}$$

$$\ddot{\chi} + C \dot{\chi} + K \chi + \delta \dot{\omega} = \mathbf{0} \tag{3}$$

where  $\tau \in \mathcal{R}^3$  is the actual control torque, and  $\tau_d \in \mathcal{R}^3$  is the external disturbance.  $\chi \in \mathcal{R}^N$  is the modal coordinate vector with respect to the

rigid part of the spacecraft, where  $N \in \mathcal{R}$  is the considered number of the elastic modes. The matrix  $\delta \in \mathcal{R}^{N \times 3}$  refers to the coupling between the flexible structures and the main body. The matrices  $\mathbf{K} = \text{diag}([\Lambda_1^2, \Lambda_2^2, \dots, \Lambda_N^2]^T) \in \mathcal{R}^{N \times N}$  and  $\mathbf{C} = \text{diag}([2\xi_1\Lambda_1, 2\xi_2\Lambda_2, \dots, 2\xi_N\Lambda_N]^T) \in \mathcal{R}^{N \times N}$  are the stiffness and damping, respectively;  $\Lambda_i \in \mathcal{R}$  is the natural frequencies, and  $\xi_i \in \mathcal{R}$  is the damping ratios,  $i = 1, 2, \dots, N$ . Moreover, the matrix  $\mathbf{R}(\theta) \in \mathcal{R}^{3 \times 3}$  and the vector  $\omega_c(\theta) \in \mathcal{R}^3$  are given by

$$\mathbf{R}(\theta) = \begin{bmatrix} 1 & 0 & -\sin \phi \\ 0 & \cos \theta & \sin \theta \cos \phi \\ 0 & -\sin \theta & \cos \theta \cos \phi \end{bmatrix} \tag{4}$$

$$\omega_c(\theta) = \omega_0 \begin{bmatrix} \cos \phi \sin \psi \\ \cos \theta \cos \psi + \sin \theta \sin \phi \sin \psi \\ -\sin \theta \cos \psi + \cos \theta \sin \phi \sin \psi \end{bmatrix} \tag{5}$$

### 2.2 Modeling of actuator uncertainty

In practice, actuator may have uncertainty. Nonnominal behavior may be seen in actuator. This uncertainty would yield performance deterioration or system instability. Let the commanded/nominal torque of actuator be denoted as  $\tau_A \in \mathcal{R}^3$ .  $\tau_F \in \mathcal{R}^3$  represents the uncertainty torque. Then, the relationship between  $\tau_A$  and  $\tau$  can be mathematically modeled as

$$\tau = \tau_A + \tau_F \tag{6}$$

### 2.3 Problem formulation

Suppose that the considered flexible spacecraft have attitude sensor and gyros to measure the attitude  $\theta$  and the angular velocity  $\omega$ . Then, the control problem of this paper can be formulated as: Applying the feedback of states' measurement  $\theta$  and  $\omega$ , design a controller for  $\tau_A$  to ensure that the attitude angles  $\theta$  is stabilized to  $\mathbf{0}$  after a fixed-time  $t_F \in \mathcal{R}_+$  despite the external disturbance  $\tau_d$ , the uncertain inertia  $\Delta \mathbf{J}$ , and the actuator uncertainty  $\tau_F$ , i.e.,  $\theta(t) \equiv \mathbf{0}$  for  $t \geq t_F$ . Moreover,  $t_F$  should be independent of the initial attitude and angular velocity.

Actually, the attitude control system (1)–(4) with actuator uncertainty (6) can be combined as

$$\begin{aligned} & \mathbf{M}(\theta)\ddot{\theta} + \mathbf{C}_1(\theta, \dot{\theta})\dot{\theta} + \mathbf{C}_2(\theta, \dot{\theta}) \\ & = \bar{\mathbf{u}}(\theta) + \bar{\mathbf{d}}(\theta, \chi) \end{aligned} \tag{7}$$

where  $\bar{\mathbf{d}}(\theta, \chi, \omega) = \mathbf{R}^T(\theta)(\tau_d + \tau_F - \Delta \mathbf{J}\dot{\omega} - \omega^\times \Delta \mathbf{J}\omega - \omega^\times \delta^T \dot{\chi} - \delta^T \ddot{\chi})$ ,  $\mathbf{M}(\theta) = \mathbf{R}^T(\theta) \mathbf{J}_0 \mathbf{R}(\theta)$ ,  $\mathbf{C}_1(\theta, \dot{\theta}) = \mathbf{R}^T(\theta) \left( \mathbf{J}_0 \frac{d\mathbf{R}(\theta)}{dt} - \omega^\times \mathbf{J}_0 \mathbf{R}(\theta) \right)$ ,  $\bar{\mathbf{u}}(\theta) = \mathbf{R}^T(\theta) \tau_A$ , and  $\mathbf{C}_2(\theta, \dot{\theta}) = -\mathbf{R}^T(\theta) \left( \mathbf{J}_0 \frac{d\omega_c(\theta)}{dt} - \omega^\times \mathbf{J}_0 \omega_c(\theta) \right)$ .

Defining  $x_1 \triangleq [x_{11}, x_{12}, x_{13}]^T = \theta$  and  $x_2 \triangleq [x_{21}, x_{22}, x_{23}]^T = \dot{\theta}$ , the system (7) can be transformed into

$$\begin{cases} \dot{x}_1 = x_2 \\ \dot{x}_2 = \mathbf{u}(x_1) + \mathbf{d}(x_1, \chi, \omega) \\ \quad - \mathbf{M}^{-1}(x_1)(\mathbf{C}_1(x_1, x_2)x_2 + \mathbf{C}_2(x_1, x_2)) \end{cases} \tag{8}$$

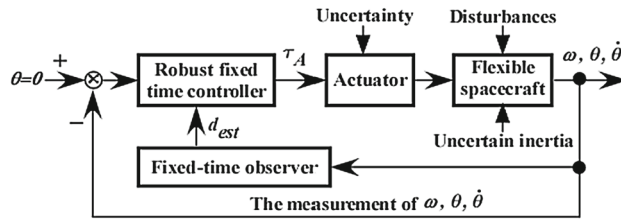
where  $x_1$  and  $x_2$  are the system states,  $\mathbf{d}(x_1, \chi, \omega) = \mathbf{M}^{-1}(\theta)\bar{\mathbf{d}}(\theta, \chi, \omega)$  denotes the lumped uncertainty, and  $\mathbf{u}(x_1) = \mathbf{M}^{-1}(\theta)\bar{\mathbf{u}}(\theta)$  is the transformed control input.

*Remark 1* Because the attitude  $\theta$  and the angular velocity  $\omega$  are measurable, it can be obtained from (1) that the states  $x_1$  and  $x_2$  of the transformed system (8) are measurable.

## 3 Main results

In this section, an observer-based fixed-time control framework is presented for flexible spacecraft attitude system to improve the convergence rate and the pointing accuracy. This control framework is developed by using the measurements of the attitude  $\theta$  and the angular velocity  $\omega$  or  $\dot{\theta}$ . Moreover, it consists of a fixed-time observer and a robust fixed-time attitude stabilization controller. The fixed-time observer is to estimate the lumped uncertainty  $\mathbf{d}$ . The states measurements and the estimated information  $\mathbf{d}_{\text{est}}$  are feedback to develop the robust fixed-time attitude stabilization controller to achieve the closed-loop system's fixed-time stability. The closed-loop attitude stabilization system resulted from this control framework is shown in Fig. 2.

**Fig. 2** The closed-loop attitude stabilization system resulted from the presented control framework



### 3.1 Development of a stable system with faster fixed-time convergence

Before the observer-based attitude control design, a fixed-time stable system is developed as

$$\dot{y} = -\xi(y) (\alpha y^p + \beta y^\lambda)^k, \quad y \in \mathcal{R}, y_0 = y(0) \quad (9)$$

where  $a > 1, b \in \mathcal{R}_+, c \in \mathcal{R}_+, \alpha \in \mathcal{R}_+, \beta \in \mathcal{R}_+, p \in \mathcal{R}_+, q \in \mathcal{R}_+,$  and  $k \in \mathcal{R}_+$  are scalars.  $pk < 1, qk > 1, \xi(y) = a + (1 - a) \exp(-b \|y\|^c),$  and  $\lambda = \frac{1}{2k} + \frac{1}{2}q + (\frac{1}{2}q - \frac{1}{2k}) \operatorname{sgn}(\|y\| - 1).$

**Lemma 1** For any initial value  $y_0,$  the system (9) is fixed-time stable, and its settling time is  $T_1 \in \mathcal{R}_+,$  i.e.,  $y(t) \equiv 0$  for  $t \geq T_1,$  where  $T_1$  is bounded as

$$T_1 < \frac{1}{\beta^k (qk - 1)} + \frac{1}{\beta^k (1 - pk)} \ln \left( 1 + \left( \frac{\beta}{\alpha} \right)^k \right) \quad (10)$$

Moreover, the convergence rate is faster than the fixed-time stable system proposed in [39].

*Proof* Please refer to ‘‘Appendix A’’. □

Lemma 1 is fundamental to the development of the subsequent observer and controller. The subsequent fixed-time observer, sliding surface, and attitude controller are developed based on it; moreover, the system stability will be analyzed by using Lemma 1. Indeed, this fixed-time stable system introduces a time-varying gain to significantly improve convergence speed near and even far away from the origin. Thus, it is expected that the observer-based attitude control possesses fast and fixed-time convergence property.

### 3.2 Fixed-time observer design for uncertainty

The transformed system (8) can be rewritten as

$$\dot{x}_2 = -l_1 x_2 + d_l + u \quad (11)$$

where  $d_l = -M^{-1}(x_1)(C_1(x_1, x_2)x_2 + C_2(x_1, x_2)) + l_1 x_2 + d$  and  $l_1 \in \mathcal{R}^+$  is a positive gain.

For (11), an auxiliary system is introduced as

$$\dot{x}_a = -l_1 x_a + u \quad (12)$$

where  $x_a \in \mathcal{R}^3$  represents the state of this auxiliary system.

Let the error between  $x_2$  and  $x_a$  be defined as  $z = x_2 - x_a,$  it leaves the dynamics of the error be the following linear system.

$$\begin{cases} \dot{z} = -l_1 z + d_l \\ y = l_2 z \end{cases} \quad (13)$$

where  $l_2 \in \mathcal{R}_+$  is a positive constant,  $z$  is the system’s state,  $y \in \mathcal{R}^3$  is the system’s output, and  $d_l$  is the unknown input of this system.

Let the fixed-time nonlinear observer for the lumped uncertainty be designed as

$$\begin{aligned} \dot{\hat{z}} = & \frac{\dot{y}}{l_2} + l_3 y - l_2 l_3 \hat{z} + \xi(e)^{\frac{1}{k_1}} \left( \alpha_1 \operatorname{sig}(e)^{\frac{2p_1 k_1 - 1}{k_1}} \right. \\ & \left. - \beta_1 \operatorname{sig}(e)^{\frac{2\lambda_1 k_1 - 1}{k_1}} \right)^{k_1} \end{aligned} \quad (14)$$

where  $l_3 \in \mathcal{R}_+, \alpha_1 \in \mathcal{R}_+, \beta_1 \in \mathcal{R}_+, p_1 \in \mathcal{R}_+, q_1 \in \mathcal{R}_+, a_1 \geq 1, b_1 \in \mathcal{R}_+, c_1 \in \mathcal{R}_+,$  and  $k_1 \in \mathcal{R}_+$  are observer gains.  $\xi(e) = a_1 + (1 - a_1) \exp(-b_1 \|e\|^{c_1}),$   $\lambda_1 = \frac{1}{2k_1} + \frac{1}{2}q_1 + (\frac{1}{2}q_1 - \frac{1}{2k_1}) \operatorname{sgn}(\|e\| - 1),$   $\hat{z}$  is the estimation of  $z,$  and  $e = z - \hat{z}$  is the estimation error. Moreover,  $\dot{y}$  is the time derivative of  $y.$

**Theorem 1** *The proposed observer (14) ensures the estimation error  $\mathbf{e}$  to be fixed-time stable, i.e.,  $\mathbf{e}(t) \equiv \mathbf{0}$  for  $t \geq T_e$ , where  $T_e$  satisfies*

$$T_e < \frac{1}{\mu_2^{k_1} (q_1 k_1 - 1)} + \frac{1}{\mu_2^{k_1} (1 - p_1 k_1)} \ln \left( 1 + \left( \frac{\mu_2}{\mu_1} \right)^{k_1} \right) \tag{15}$$

where  $\mu_1 = 2^{p_1} \alpha_1$  and  $\mu_2 = 2^{\lambda_1} \beta_1$ .

*Proof* Please refer to ‘‘Appendix B’’. □

**Theorem 2** *Let an estimation law  $\mathbf{d}_{\text{est}}$  be designed as*

$$\mathbf{d}_{\text{est}} = \hat{\mathbf{d}}_l - l_1 \mathbf{x}_2 + \mathbf{M}^{-1}(\mathbf{x}_1) (\mathbf{C}_1(\mathbf{x}_1, \mathbf{x}_2) \mathbf{x}_2 + \mathbf{C}_2(\mathbf{x}_1, \mathbf{x}_2)) \tag{16}$$

where

$$\hat{\mathbf{d}}_l = \frac{l_1 l_2 \hat{\mathbf{z}} + \dot{\mathbf{y}}}{l_2} \tag{17}$$

Then, the lumped uncertainty  $\mathbf{d}$  is precisely estimated by  $\mathbf{d}_{\text{est}}$  within a fixed time  $T_e$ . The estimation error  $\mathbf{d}_e = \mathbf{d} - \mathbf{d}_{\text{est}}$  is such that  $\mathbf{d}_e(t) \equiv \mathbf{0}$  for  $t \geq T_e$ .

*Proof* Please refer to ‘‘Appendix C’’. □

**Remark 2** It is seen in Theorem 1 and Theorem 2 that  $\dot{\mathbf{y}}$  is required to implement the proposed control approach in practice. To satisfy this requirement, the high-order sliding-mode differentiators (HOSMDs) [41] can be applied to obtain  $\dot{\mathbf{y}}$ . That is because the HOSMDs can achieve an exact and finite-time estimation of the required  $\dot{\mathbf{y}}$  by inputting the signal value  $\mathbf{y}$  into the differentiator. It is seen in [41] that a  $K$  th-order sliding-mode differentiator ( $K > 2$ ) has a form of

$$\begin{cases} \dot{\chi}_0 = v_0, v_0 = \chi_1 - \kappa_0 \|\chi_0 - \mathbf{h}\|^{\frac{\kappa_0}{\kappa_0+1}} \text{sig}(\chi_0 - \mathbf{h})^0 \\ \dot{\chi}_j = v_j, v_j = \chi_{j+1} - \kappa_j \|\chi_j - v_{j-1}\|^{\frac{\kappa_j}{\kappa_j+1}} \text{sig}(\chi_j - v_{j-1})^0 \\ \vdots \\ j = 1, 2, \dots, K-1 \\ \dot{\chi}_K = -\kappa_K \text{sig}(\chi_K - v_{K-1})^0 \end{cases} \tag{18}$$

where  $\kappa_j \in \mathcal{R}_+$  is positive gains,  $\chi_j \in \mathcal{R}^r$  is the state of this differentiator,  $j = 1, 2, \dots, K$ ,  $\mathbf{h} \in \mathcal{R}^r$  is the

input signal. Following Theorem 5 in [41],  $\dot{\mathbf{h}} = \mathbf{v}_0$  is achieved after a finite time. Hence, when applying the differentiator (18) to calculate  $\dot{\mathbf{y}}$ ,  $\mathbf{y}$  should be chosen as the input signal  $\mathbf{h}$ , i.e.,  $\mathbf{h} = \mathbf{y}$ , and  $\chi_j \in \mathcal{R}^3$ ,  $j = 1, 2, \dots, K$ . Then, it follows that  $\dot{\mathbf{y}} = \mathbf{v}_0$ .

**Remark 3** It is seen in Remark 1 and the first paragraph in Sect. 2.3 that  $\boldsymbol{\theta}$ ,  $\boldsymbol{\omega}$ ,  $\dot{\boldsymbol{\theta}}$ ,  $\mathbf{x}_1$ , and  $\mathbf{x}_2$  are measurable via the sensors fixed in the considered spacecraft. Moreover,  $\mathbf{x}_a$  can be obtained by solving (12) for any  $\mathbf{u}$ . Then,  $\mathbf{z}$  can be numerically obtained, and  $\hat{\mathbf{z}}$  is available from (14). Therefore, the observer (14) is available for practical implementation. In addition, it is known from the paragraph below (7) and the nominal inertia  $\mathbf{J}_0$  that  $\mathbf{M}^{-1}(\mathbf{x}_1)$ ,  $\mathbf{C}_1(\mathbf{x}_1, \mathbf{x}_2)$ , and  $\mathbf{C}_2(\mathbf{x}_1, \mathbf{x}_2)$  are available. Consequently, it can be obtained from Remark 2 and (17) that the estimation  $\mathbf{d}_{\text{est}}$  is also available.

### 3.3 Development of a fixed-time sliding manifold

The following fixed-time sliding manifold  $\mathcal{S}$  (FTSM) is synthesized to circumvent the singularity issue and provide the system states with fast fixed-time convergence.

$$\mathcal{S} = \mathbf{H}(\mathbf{x}_1) \mathbf{x}_1 + \text{sig}^\gamma(\mathbf{x}_2) \tag{19}$$

with  $\mathbf{H}(\mathbf{x}_1) = \text{diag}([h(x_{11}), h(x_{12}), h(x_{13})]^T)$  and

$$h(x_{1i}) = \left( \xi(\mathbf{x}_1)^{\frac{1}{k_2}} \alpha_2 |x_{1i}|^{p_2 - \frac{1}{k_2 \gamma}} + \xi(\mathbf{x}_1)^{\frac{1}{k_2}} \beta_2 |x_{1i}|^{\lambda_2 - \frac{1}{k_2 \gamma}} \right)^{k_2 \gamma}, i = 1, 2, 3 \tag{20}$$

where  $\alpha_2 \geq 1$ ,  $\alpha_2 \in \mathcal{R}_+$ ,  $\beta_2 \in \mathcal{R}_+$ ,  $p_2 \in \mathcal{R}_+$ ,  $q_2 \in \mathcal{R}_+$ ,  $k_2 \in \mathcal{R}_+$ ,  $\gamma > 1$ ,  $b_2 \in \mathcal{R}_+$ , and  $c_2 \in \mathcal{R}_+$  are constants.  $1/\gamma < p_2 k_2 < 1$ ,  $q_2 k_2 > 1$ ,  $\lambda_2 = \frac{1}{2k_2} + \frac{1}{2} q_2 + \left(\frac{1}{2} q_2 - \frac{1}{2k_2}\right) \text{sgn}(\|\mathbf{x}_1\| - 1)$ , and  $\xi(\mathbf{x}_1) = a_2 + (1 - a_2) \exp(-b_2 \|\mathbf{x}_1\|^{c_2})$ .

**Theorem 3** *If a control law can be presented to govern the states of the attitude system to reach  $\mathcal{S} = \mathbf{0}$  and stay in thereafter, then the system states converge to  $\mathbf{0}$  after a fixed time  $T_s \in \mathcal{R}_+$ , which does not depend on the initial states. Moreover,  $T_s$  is bounded as*

$$T_s < \frac{1}{\beta_2^{k_2} (q_2 k_2 - 1)}$$

$$+ \frac{1}{\beta_2^{k_2} (1 - p_2 k_2)} \ln \left( 1 + \left( \frac{\beta_2}{\alpha_2} \right)^{k_2} \right) \tag{21}$$

*Proof* Please refer to ‘‘Appendix D’’. □

*Remark 4* In [29, 42], a fixed-time sliding manifold has been presented as (19) in which  $h(x_{1i})$  is expressed as

$$h(x_{1i}) = \left( \alpha_2 |x_{1i}|^{p_2 - \frac{1}{k_2 \gamma}} + \beta_2 |x_{1i}|^{q_2 - \frac{1}{k_2 \gamma}} \right)^{k_2 \gamma} \tag{22}$$

The fixed time ensured by [29, 42] is bounded by  $\bar{T}_x \leq \frac{1}{\beta_2^{k_2} (q_2 k_2 - 1)} + \frac{1}{\alpha_2^{k_2} (1 - p_2 k_2)}$ . Since  $\ln \left( 1 + \left( \frac{\beta_2}{\alpha_2} \right)^{k_2} \right) \leq \left( \frac{\beta_2}{\alpha_2} \right)^{k_2}$  always holds, the proposed FTSM of this paper obtains faster convergence rate than the FTSM presented by [42].

### 3.4 Robust fixed-time attitude controller design

Let the robust fixed-time attitude stabilization controller be synthesized as

$$\begin{aligned} \tau_A = & (R^T(\theta))^{-1} M(\theta) (M^{-1}(x_1) (C_1(x_1, x_2) x_2 \\ & + C_2(x_1, x_2)) - \frac{1}{\gamma} (\tilde{H}(x_1) + H(x_1)) \text{sig}(x_1)^{2-\gamma} \\ & - d_{\text{est}} - \frac{1}{\rho_0 \gamma} P(x_2) (\xi(S)^{1/k_3} \alpha_3 \text{sig}(S)^{(2p_3 k_3 - 1)/k_3} \\ & + \xi(S)^{1/k_3} \beta_3 \text{sig}(S)^{(2\lambda_3 k_3 - 1)/k_3})^{k_3} \end{aligned} \tag{23}$$

where  $P(x_2) = \text{diag}([\mu_\sigma (|x_{21}|^{\gamma-1}) |x_{21}|^{\gamma-1}, \mu_\sigma (|x_{22}|^{\gamma-1}) \times |x_{22}|^{\gamma-1}, \mu_\sigma (|x_{23}|^{\gamma-1}) |x_{23}|^{\gamma-1}]^T)$ .  $k_3 > 1$ ,  $\alpha_3 4 \in \mathcal{R}_+$ ,  $\beta_3 \in \mathcal{R}_+$ , and  $\rho_0 = \pi / (2\sigma)$  are control gains.  $p_3 k_3 < 1$ ,  $q_3 k_3 > 1$ , and  $\tilde{H}(x_1) = \text{diag}[\tilde{h}(x_{11}), \tilde{h}(x_{12}), \tilde{h}(x_{13})]^T$ ,  $i = 1, 2, 3$ ,

$$\begin{aligned} \tilde{h}(x_{1i}) = & k_1 \gamma \left( \xi(x_1)^{1/k_2} \alpha_2 |x_{1i}|^{p_2 - \frac{1}{k_2 \gamma}} \right. \\ & \left. + \xi(x_1)^{1/k_2} \beta_2 |x_{1i}|^{\lambda_2 - \frac{1}{k_2 \gamma}} \right)^{k_2 \gamma - 1} \\ & \times \left( \xi(x_1)^{1/k_2} \alpha_2 \left( p_2 - \frac{1}{k_2 \gamma} \right) |x_{1i}|^{p_2 - \frac{1}{k_2 \gamma}} \right. \\ & \left. + \xi(x_1)^{1/k_2} \beta_2 \left( \lambda_2 - \frac{1}{k_2 \gamma} \right) |x_{1i}|^{\lambda_2 - \frac{1}{k_2 \gamma}} \right) \end{aligned} \tag{24}$$

Moreover, the function  $\mu_\sigma$  is

$$\mu_\sigma(x) = \begin{cases} \sin(0.5\pi x/\sigma), & |x| \leq \sigma \\ 1, & |x| > \sigma \end{cases} \tag{25}$$

**Theorem 4** For the flexible spacecraft with the external disturbance  $\tau_d$ , the uncertain inertia  $\Delta J$ , and the actuator uncertainty  $\tau_F$ , applying the estimation law (14) and the fixed-time attitude controller (23), then the attitude Euler angles and the rotation velocity are fixed-time stable with the settling time  $T_c$  satisfying  $T_c < T_s + T_1$ , where  $T_1$  is bounded by

$$T_1 < \frac{1}{\mu_4^{k_3} (q_3 k_3 - 1)} + \frac{1}{\mu_4^{k_3} (1 - p_3 k_3)} \ln \left( 1 + (\mu_4 / \mu_3)^{k_3} \right) \tag{26}$$

where  $\mu_3 = \alpha_3 \rho_0^{-1/k_3} \mu_\sigma^{1/k_3} (|x_{2i}|^{\gamma-1})$  and  $\mu_4 = \beta_3 \rho_0^{-1/k_3} \times \mu_\sigma^{1/k_3} (|x_{2i}|^{\gamma-1})$ .

*Proof* Please refer to ‘‘Appendix E’’. □

*Remark 5* In contrast to the existing observers, the proposed observer (16) provides precise estimation for the lumped uncertainty after a fixed time which does not depend on the initial estimation error. The estimation error is zero after that fixed time. Moreover, it relaxes some assumptions such as the need for upper limit of total uncertainties to be available in advance or the time derivative of the disturbance to converge to zero. This is one of the main contributions of this work.

*Remark 6* When practically implement the proposed approach to perform attitude maneuver, the controller (23) and the observer (14) will be numerically computed by the spacecraft’s onboard embedded computer. The designed control scheme is hence implementable for in-orbital spacecraft. Moreover, the procedures to choose the control gains are listed in the following Remark 7. Hence, the controller is practically implementable for spacecraft system. This is validated in Sect. 4 with simulation results presented.

*Remark 7* When implementing the proposed approach, control gains  $\alpha_i$ ,  $\beta_i$ ,  $p_i$ ,  $q_i$ ,  $k_i$ ,  $a_j$ , and  $b_j$  ( $i = 1, 2, 3$ ,  $j = 1, 2$ ) should be carefully chosen and tuned to achieve higher attitude accuracy and acceptable control power. Based on (21) and (26), the following procedures should be followed for choice of the control gains.

- (a) Larger  $\alpha_i$  and  $\beta_i$  lead to a faster convergence rate, but large overshoot and more control energy consumption will be resulted. Hence, a compromise should be made between the converging rate and the overshoot.
- (b) According to (21) and (26), the gains  $p_i$ ,  $q_i$ , and  $k_i$  are also important to determine the system's converging rate.
- (c) The gains  $a_j$  and  $b_j$  have profound influence on the convergence rate. If  $a_j$  is selected near to 1, the effect of  $\xi$  is reduced, and vice versa. By choosing  $b_j$  large enough, the impact of  $\xi$  is highlighted.

#### 4 Simulation results

To validate the superior attitude control performance of the presented approach, numerical simulation is conducted on a flexible spacecraft with its structure shown in Fig. 1. The details of this spacecraft is provided in [43]. The task of this spacecraft is Earth observation. The spacecraft's orbit is circular. Its altitude and inclination are 638 km and 95.4 degrees, respectively, i.e.,  $\omega_0 = 0.0011$  rad/s. As shown in Fig. 1, there are two solar paddles fixed in the  $+Y_B$  and the  $-Y_B$  axis, respectively. They are called the north and the south solar paddle, receptively. Each paddle has a dimension of  $15 \times 0.75$  m. The nominal designed inertia of

the spacecraft is  $J_0 = \begin{bmatrix} 487 & 15 & -1.2 \\ 14.9 & 177 & -7.3 \\ -1.2 & -7.3 & 404 \end{bmatrix} \text{ kg} \cdot \text{m}^2$ .

After ground testing, the coupling matrix between the rigid body and the solar paddles is calculated as  $\delta = \begin{bmatrix} 1 & 0.1 & 0.1 \\ 0.5 & 0.1 & 0.01 \\ -1 & 0.3 & 0.01 \end{bmatrix} \text{ kg} \cdot \text{m}^2$ . Moreover, it is tested that when choosing the elastic mode number  $N$  as  $N = 3$ , the flexible vibration of solar paddles can be mainly reflected. Hence,  $N = 3$  is chosen to establish the model of the attitude control system. Correspondingly, the natural frequencies are measured as  $\Lambda_1 = 1.8912$  rad/sec,  $\Lambda_2 = 2.884$  rad/sec,  $\Lambda_3 = 3.4181$  rad/sec, respectively. The damping ratios are measured on the ground as  $\xi_1 = \xi_2 = \xi_3 = 0.01$ .

For the considered spacecraft, the gravity-gradient torque, the aerodynamic torque, and the Earth magnetic torque are the primary external disturbances for  $\tau_d$  in (2), which will be considered in simulation. They will

be mathematically calculated according to [40] and put into the system model. Moreover, the uncertain inertia is assumed to be  $\Delta J = 0.1 J_0$ . When carrying out simulation, the initial attitude are  $\psi(0) = 15$  degrees,  $\phi(0) = 25$  degrees, and  $\theta(0) = -5$  degrees. The initial velocity is  $\omega(0) = [0.01, -0.01, -0.02]^T$  rad/s.

Besides the proposed observer-based fast fixed-time attitude control (named as OBFFTAC), the fixed-time attitude control presented in [29] (denoted by FTAC) is also simulated under the same condition for performance comparison. For fair comparison, the parameters of OBFFTAC is taken the same as FTAC except for the new parameters in the sliding manifold as well as the controller. The OBFFTAC parameters are chosen as  $\gamma = 1.5$ ,  $p_1 = 0.35$ ,  $p_2 = 0.3$ ,  $p_3 = 0.45$ ,  $q_1 = 0.6$ ,  $q_2 = 0.75$ ,  $q_3 = 0.45$ ,  $\alpha_1 = 0.2$ ,  $\alpha_2 = 0.1$ ,  $\alpha_3 = 0.4$ ,  $\beta_1 = 0.08$ ,  $\beta_2 = 0.06$ ,  $\beta_3 = 0.1$ ,  $k_1 = 2$ ,  $k_2 = 2$ ,  $k_3 = 2$ ,  $l_1 = 0.02$ ,  $l_2 = 14$ ,  $l_3 = 25$ ,  $\sigma = 0.01$ ,  $a_1 = 1.4$ ,  $a_2 = 1.35$ ,  $b_1 = 6$ ,  $b_2 = 4$ , and  $c_1 = c_2 = 1$ . Moreover, the fifth-order sliding-mode differentiator (18) is used to calculate  $\dot{y}$  with  $K = 5$  and  $\kappa_0 = \kappa_1 = \kappa_2 = \kappa_3 = \kappa_4 = \kappa_5 = 1.5$ .

##### 4.1 Comparison in the case of normal actuators

In the subsection, the case that all the actuators of the flexible spacecraft do not have any uncertainty is considered. For this case, the resulted attitude stabilization results from the OBFFTAC and the FTAC are illustrated in Figs. 3, 4, 5. It is found that the OBFFTAC achieves faster converging rate and higher pointing accuracy, while the maximum required control torques are almost identical. To provide further insight into the control performance in terms of pointing accuracy as well as the convergence rate, the data analysis is given in Table 1. It is found that the OBFFTAC provides faster convergence rate and smaller steady-state error. The improvement percentage confirms the superior performance of OBFFTAC especially in terms of pointing accuracy. Moreover, the norm of the attitude angles and the rotation velocity are shown in Figs. 6 and 7, respectively. That two controllers successfully accomplish the planned attitude maneuvering. However, the OBFFTAC provides greatly preferable control performance to the FTAC both in theory and simulation.



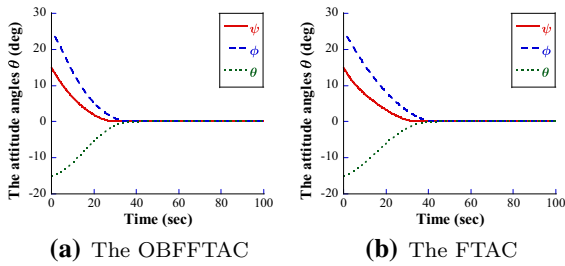


Fig. 3 The attitude angles in the case of normal actuators

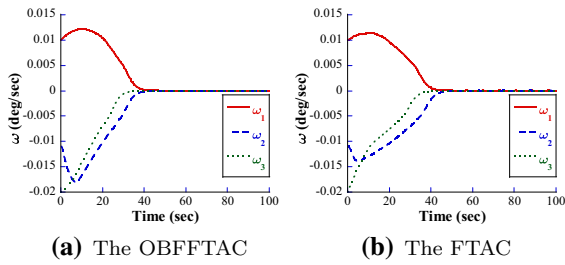


Fig. 4 The angular velocity in the case of normal actuators

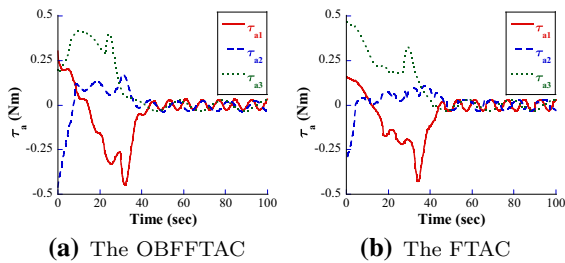


Fig. 5 The control torque in the case of normal actuators

4.2 Comparison in the case of actuator uncertainty

To evaluate the robust control capability of the controllers, actuator uncertainty is considered in this case. In particular, the actuator uncertainty is assumed to be the actuator fault:

$$\tau_F = (G(t) - I_3)\tau_A + \bar{\tau} \tag{27}$$

where  $G(t) = \text{diag}([g_1, g_2, g_3]^T)$  refers to the actuator effectiveness matrix in which  $g_i$  represents fault indicator of the  $i$ th actuator,  $\bar{\tau} = [\bar{\tau}_1, \bar{\tau}_2, \bar{\tau}_3]^T$  denotes the bias fault. For example,  $g_i = 1$  and  $\bar{\tau}_i = 0$  is associated with the case that  $i$ th actuator is healthy.  $0 < g_i < 1$  denotes that the  $i$ th actuator partially rather than totally loses its control effectiveness.

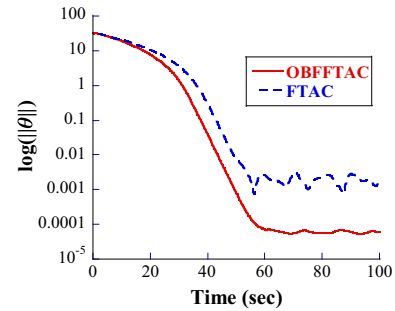


Fig. 6 Norm of the attitude angles in the case of normal actuators

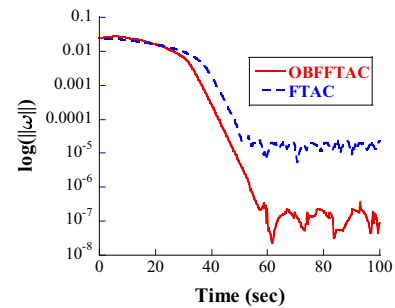


Fig. 7 Norm of the angular velocity in the case of normal actuators

In this subsection, the fault indicator and bias faulty torque are given as  $\bar{\tau}_1 = 0.6\text{Nm}$ ,  $\bar{\tau}_2 = -0.03\text{Nm}$ ,  $\bar{\tau}_3 = 0.05\text{Nm}$ ,  $g_1 = \begin{cases} 1, & \text{if } t \leq 20 \\ 0.5, & \text{otherwise} \end{cases}$ ,  $g_2 = \begin{cases} 1, & \text{if } t \leq 35 \\ 0.6, & \text{otherwise} \end{cases}$ , and  $g_3 = \begin{cases} 1, & \text{if } t \leq 25 \\ 0.5, & \text{otherwise} \end{cases}$ , when conducting simulation. Moreover, all the control gains are chosen the same as given in the preceding case.

Figures 8 and 9 illustrate the attitude and the rotation velocity revealing that the OBFFTAC obtains much faster convergence rate for the case of having actuator uncertainty. The control performance is considerably degraded under the FTAC. The convergence time obtained by the FTAC significantly increases because of its longer rotation path.

According to Figs. 10 and 11, it can be concluded that the OBFFTAC obtains the most accurate attitude control. This is due to the observer-based estimation law (16). The comparison result is listed in Table 2. The proposed strategy, in contrast to the FTAC, successfully deals with the actuator uncertainty. It is confirmed that the control performance of the FTAC was

**Table 1** Performance comparison in the case of normal actuators

Controller	Euler angles	Angular velocity	Convergence time*
OBFFTAC	$5.5 \times 10^{-6}$	$4 \times 10^{-7}$	44.6
FTAC	$4 \times 10^{-3}$	$3 \times 10^{-5}$	51.2
Improvement percentage, %	98.25	98.67	12.89

\*The convergence time is defined as the time after which  $\|\theta\| \leq 6 \times 10^{-3}$  (deg) and  $\|\omega\| \leq 4 \times 10^{-5}$ (deg/s) are satisfied

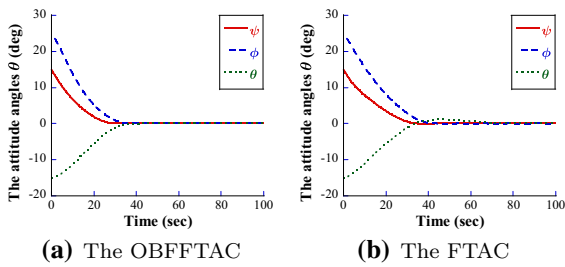


**Fig. 8** The attitude angles in the case of actuator uncertainty

significantly deteriorated while the actuators experienced uncertainty. The attitude control results of the OBFFTAC are roughly similar to that of the previous case. However, the FTAC failed to drive the attitude angles and the rotation velocity to the desired region. The superiority of the OBFFTAC over the FTAC was highlighted by this scenario.

The control power consumed is shown in Fig. 12. The maximum required control efforts for that two controllers are almost identical showing the superior control performance of the OBFFTAC. The lumped uncertainties along with their estimations are illustrated in Fig. 13. It is observed from the estimation errors in Fig. 14 that the total uncertainties are precisely reconstructed in a finite time, which is independent of the initial estimation errors. When a sudden actuator failure happened, the observer successfully estimated it to preserve stability and control performance. Such results confirm the claims presented in Theorem 3 that the suggested estimation law can estimate the lumped uncertainties in a fixed time. This is also the reason that superiority can be obtained from the OBFFTAC.

**5 Conclusion**

Although there exist several approaches regarding flexible spacecraft attitude control with accurate pointing, few can achieve fixed-time convergence of the system

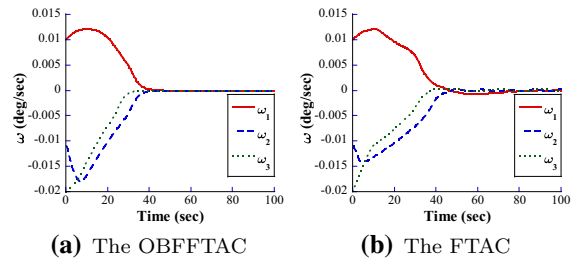


**Fig. 9** The angular velocity in the case of actuator uncertainty

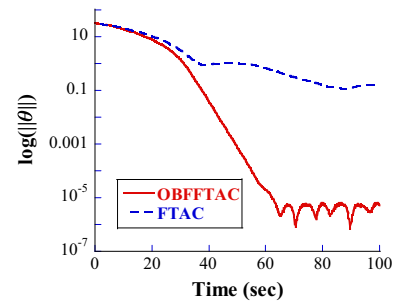


**Fig. 10** Norm of the attitude angles in the case of actuator uncertainty

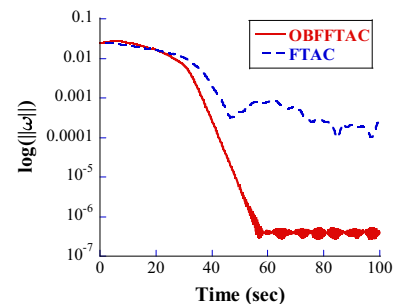


**Fig. 11** Norm of the angular velocity in the case of actuator uncertainty

states in the face of actuator uncertainty. This work presented an estimation-based strategy for flexible spacecraft attitude stabilization maneuvering. In particular, the control law incorporated a fast fixed-time observer for reconstructing the uncertain dynamics, and a robust

**Table 2** Performance comparison in the case of actuator uncertainty

Controller	Euler angles	Angular velocity	Convergence time*
OBFFTAC	$7 \times 10^{-6}$	$6 \times 10^{-7}$	44.6
FTAC	0.2	$4 \times 10^{-4}$	$\infty$
Improvement percentage, %	99.99	99.85	100

\*The convergence time is defined as the time after which  $\|\theta\| \leq 6 \times 10^{-3}$  (deg) and  $\|\omega\| \leq 4 \times 10^{-5}$ (deg/s) are satisfied

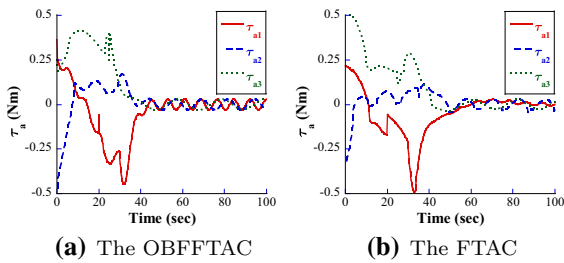


**Fig. 12** The control torques in the case of actuator uncertainty

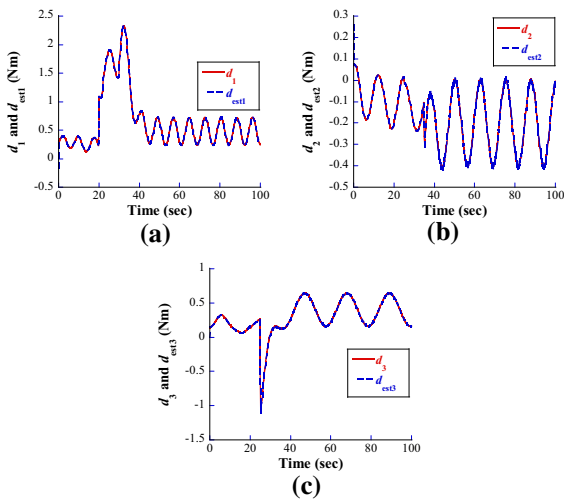


**Fig. 13** Uncertain dynamics and its estimation in the case of actuator uncertainty

fixed-time controller. This was developed via a nonsingular terminal sliding mode surface providing a faster converging rate when compared to the existing fixed-time surfaces.

It should be stressed that a faster convergence rate leads to more control power. Actuator saturation may occur. This issue should be explicitly addressed in the future. Otherwise, system instability may be resulted.

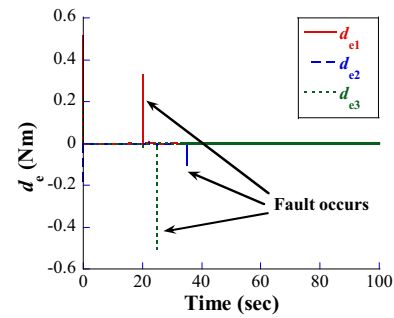


**Fig. 14** The estimation error of the uncertainty in the case of actuator uncertainty

Moreover, considering measurement noise, robust controller should also be designed.

**Compliance with ethical standards**

**Conflict of interest** The authors declare that they have no conflict of interest.

**Appendix A (Proof of Lemma 1)**

Defining a new variable  $W = y^{1-pk}$ , it can be obtained from (9) that

$$\begin{aligned} \dot{W} &= -(1 - pk) y^{-pk} \left( \xi(y)^{\frac{1}{k}} \alpha y^p + \xi(y)^{\frac{1}{k}} \beta y^\lambda \right)^k \\ &= -(1 - pk) \left( \xi(y)^{\frac{1}{k}} \alpha + \xi(y)^{\frac{1}{k}} \beta W^\eta \right)^k \end{aligned} \tag{28}$$

where  $\eta = \frac{\lambda-p}{1-pk}$ .

Since  $1 - pk > 0$  and  $\xi(y) > 1$ , it follows from (28) that

$$\dot{W} \leq -(1 - pk) (\alpha + \beta W^\eta)^k \tag{29}$$

Applying the result in [39] and the comparison principle [44], it can be proved from (29) that  $W$  is fixed-time stable. Moreover, solving (28), one can get the settling time as

$$\begin{aligned}
 T_1 &= \frac{1}{(1-pk)} \int_0^{W_0} \frac{1}{\left(\xi(y)^{\frac{1}{k}} \alpha + \xi(y)^{\frac{1}{k}} \beta W^\eta\right)^k} dW \\
 &= \frac{1}{(1-pk)} \left( \int_1^{W_0} \frac{1}{\xi(y) (\alpha + \beta W^{\bar{\eta}})^k} dW \right. \\
 &\quad \left. + \int_0^1 \frac{1}{\xi(y) \left(\alpha + \beta W^{\frac{1}{k}}\right)^k} dW \right)
 \end{aligned} \tag{30}$$

where  $\bar{\eta} = \frac{q-p}{1-pk}$  and  $W_0 = (y(0))^{1-pk}$ .  
 If  $\xi(y) = 1$ , then one has

$$\begin{aligned}
 T_1' &= \frac{1}{(1-pk)} \left( \int_1^{W_0} \frac{1}{(\alpha + \beta W^{\bar{\eta}})^k} dW \right. \\
 &\quad \left. + \int_0^1 \frac{1}{(\alpha + \beta W^{1/k})^k} dW \right)
 \end{aligned} \tag{31}$$

Since  $1 \leq \xi(y) \leq a$ , then  $1/a \leq 1/\xi(y) \leq 1$ . Hence, for all  $W_0$ , it is concluded that

$$T_1 < T_1' \tag{32}$$

On other hand,  $T_1'$  is also the settling time of the fixed-time system given in [39]. To this end, one can prove that the settling time provided by the proposed system (9) is less than [39]. The convergence rate of the system (9) is faster than [39].

From (30), it be proved that  $T_1'$  is bounded as

$$\begin{aligned}
 T_1' &\leq \frac{1}{(1-pk)} \left( \int_1^{W_0} \frac{1}{\beta^k W^{\bar{\eta}k}} dW + \int_0^1 \frac{1}{\alpha^k + \beta^k W} dW \right) \\
 &\leq \frac{1}{(1-pk)} \left( \frac{1 - W_0^{1-\bar{\eta}k}}{\beta^k (\bar{\eta}k - 1)} + \frac{1}{\beta^k} \ln \left( 1 + (\beta/\alpha)^k \right) \right)
 \end{aligned} \tag{33}$$

Since  $\bar{\eta}k > 1$  and  $W_0 > 0$ , one has

$$T_1' \leq \frac{1}{\beta^k (qk - 1)} + \frac{1}{\beta^k (1 - pk)} \ln \left( 1 + (\beta/\alpha)^k \right) \tag{34}$$

which does not depend on the initial condition.

### Appendix B (Proof of Theorem 1)

It is obtained from (13) and (14) that the estimation error of the observer satisfies

$$\begin{aligned}
 \dot{e} &= \dot{z} - \hat{\dot{z}} = \dot{z} + l_2 l_3 \hat{z} - \frac{1}{l_2} \dot{y} - l_3 y \\
 &\quad - \left( \xi(e)^{1/k_1} \alpha_1 \text{sig}(e)^{\frac{2p_1 k_1 - 1}{k_1}} \right. \\
 &\quad \left. + \xi(e)^{1/k_1} \beta_1 \text{sig}(e)^{\frac{2\lambda_1 k_1 - 1}{k_1}} \right)^{k_1} \\
 &= -l_2 l_3 e - \left( \xi(e)^{1/k_1} \alpha_1 \text{sig}(e)^{\frac{2p_1 k_1 - 1}{k_1}} \right. \\
 &\quad \left. + \xi(e)^{1/k_1} \beta_1 \text{sig}(e)^{\frac{2\lambda_1 k_1 - 1}{k_1}} \right)^{k_1}
 \end{aligned} \tag{35}$$

Define a Lyapunov candidate function as  $V_1 = 0.5e^T e$ , it leaves its time derivative as

$$\begin{aligned}
 \dot{V}_1 &= e^T \dot{e} \leq -e^T \left( \xi(e)^{1/k_1} \alpha_1 \text{sig}(e)^{\frac{2p_1 k_1 - 1}{k_1}} \right. \\
 &\quad \left. + \xi(e)^{1/k_1} \beta_1 \text{sig}(e)^{\frac{2\lambda_1 k_1 - 1}{k_1}} \right)^{k_1} \\
 &\leq - \sum_{i=1}^3 \left( \xi(e)^{1/k_1} \alpha_i |e_i|^{\frac{2p_1 k_1 - 1}{k_1} + \frac{1}{k_1}} \right. \\
 &\quad \left. + \xi(e)^{1/k_1} \beta_i |e_i|^{\frac{2\lambda_1 k_1 - 1}{k_1} + \frac{1}{k_1}} \right)^{k_1} \\
 &\leq - \left( \xi^{1/k_1} \mu_1 V_1^{p_1} + \xi^{1/k_1} \mu_2 V_1^{\lambda_1} \right)^{k_1}
 \end{aligned} \tag{36}$$

Applying Lemma 1 and the comparison principle [44], it is concluded that  $V(e) \equiv 0$  is met for  $t \geq T_e$ , where the settling time  $T_e$  satisfies (15).

**Appendix C (Proof of Theorem 2)**

From (16) and (17), it follows that

$$\begin{aligned} \mathbf{d}_e &= \mathbf{d}_l - l_1 \mathbf{x}_2 + \mathbf{M}^{-1}(\mathbf{x}_1) (\mathbf{C}_1(\mathbf{x}_1, \mathbf{x}_2) \mathbf{x}_2 \\ &\quad + \mathbf{C}_2(\mathbf{x}_1, \mathbf{x}_2)) - \hat{\mathbf{d}}_l + l_1 \mathbf{x}_2 \\ &\quad - \mathbf{M}^{-1}(\mathbf{x}_1) (\mathbf{C}_1(\mathbf{x}_1, \mathbf{x}_2) \mathbf{x}_2 + \mathbf{C}_2(\mathbf{x}_1, \mathbf{x}_2)) \\ &= \mathbf{d}_l - \hat{\mathbf{d}}_l \end{aligned} \tag{37}$$

Substituting (17) in (37) gives

$$\begin{aligned} \mathbf{d}_e &= \mathbf{d}_l - \frac{l_1 l_2 \hat{\mathbf{z}} + \dot{\mathbf{y}}}{l_2} \\ &= \mathbf{d}_l - \frac{l_1 l_2 \hat{\mathbf{z}} - l_1 l_2 \mathbf{z} + l_2 \mathbf{d}_l}{l_2} = l_1 \mathbf{e} \end{aligned} \tag{38}$$

Because  $\mathbf{e}(t) \equiv \mathbf{0}$  is achieved in Theorem 1 for  $t \geq T_e$ ,  $\mathbf{d}_e(t) = \mathbf{0}$  is achieved for  $t \geq T_e$ . It is inferred that  $\mathbf{d}$  is estimated utilizing  $\mathbf{d}_{est}$  after  $T_e$ .

**Appendix D (Proof of Theorem 3)**

When  $\mathbf{S} = \mathbf{0}$  is reached, from (19), one has

$$\begin{aligned} \dot{x}_{1i} &= -(h(x_{1i}))^{1/\gamma} \text{sig}^{1/\gamma}(x_{1i}) \\ &= -\left(\xi(x_1)^{1/k_2} \alpha_1 |x_{1i}|^{p_2-1/k_2\gamma} \right. \\ &\quad \left. - \xi(x_1)^{1/k_2} \beta_2 |x_{1i}|^{\lambda_2-1/k_2\gamma}\right)^{k_2} \text{sig}^{1/\gamma}(x_{1i}) \\ &= -\left(\xi(x_1)^{1/k_2} \alpha_2 |x_{1i}|^{p_2} \right. \\ &\quad \left. - \xi(x_1)^{1/k_2} \beta_2 |x_{1i}|^{\lambda_2}\right)^{k_2} \text{sgn}(x_{1i}) \end{aligned} \tag{39}$$

Defining a new variable  $\Xi_i = |x_{1i}|^{1-p_2k_2}$ , (39) is expressed as

$$\begin{aligned} \dot{\Xi}_i &= -(1 - p_2k_2) \dot{x}_{1i} |x_{1i}|^{-p_2k_2} \text{sgn}(x_{1i}) \\ &= -(1 - p_2k_2) |x_{1i}|^{-p_2k_2} \left(\xi(x_1)^{1/k_2} \alpha_2 |x_{1i}|^{p_2} \right. \\ &\quad \left. + \xi(x_1)^{1/k_2} \beta_2 |x_{1i}|^{\lambda_2}\right)^{k_2} \\ &= -(1 - p_2k_2) \left(\xi(x_1)^{\frac{1}{k_2}} \alpha_2 + \xi(x_1)^{\frac{1}{k_2}} \beta_2 \Xi_i^{\eta_2}\right)^{k_2} \end{aligned} \tag{40}$$

where  $\eta_2 = \frac{\lambda_2-p_2}{1-p_2k_2}$ . Similar to Lemma 1, the system state converges to zero after a fixed time given by (21).

**Appendix E (Proof of Theorem 4)**

Select another Lyapunov candidate function  $V_s = \mathbf{S}^T \mathbf{S}$ . Applying (8), one can calculate the time derivative of  $V_s$  as

$$\begin{aligned} \dot{V}_s &= 2\mathbf{S}^T (\dot{\mathbf{H}}(\mathbf{x}_1) \mathbf{x}_1 + \mathbf{H}(\mathbf{x}_1) \dot{\mathbf{x}}_1 \\ &\quad + \gamma \text{diag}(|x_{2i}|^{\gamma-1}) \\ &\quad \times (-\mathbf{M}^{-1}(\mathbf{x}_1) (\mathbf{C}_1(\mathbf{x}_1, \mathbf{x}_2) \mathbf{x}_2 \\ &\quad + \mathbf{C}_2(\mathbf{x}_1, \mathbf{x}_2)) \\ &\quad + \mathbf{u}(\mathbf{x}_1) + \mathbf{d}(\mathbf{x}_1, \boldsymbol{\chi}, \boldsymbol{\omega})) \end{aligned} \tag{41}$$

Substituting the controller (23) into (41) yields

$$\begin{aligned} \dot{V}_s &= \frac{2}{\rho_0} \mathbf{S}^T \text{diag}(\mu_\sigma (|x_{2i}|^{\gamma-1})) \\ &\quad \times \left(\xi^{1/k_3} \alpha_3 \text{sig}(\mathbf{S})^{(2p_3k_3-1)/k_3} \right. \\ &\quad \left. + \xi^{1/k_3} \beta_3 \text{sig}(\mathbf{S})^{(2\lambda_3k_3-1)/k_3}\right)^{k_3} \\ &\quad + \gamma \mathbf{S}^T \text{diag}(|x_{2i}|^{\gamma-1}) (\mathbf{d} - \mathbf{d}_{est}) \end{aligned} \tag{42}$$

Since  $\mathbf{d}_e = \mathbf{d} - \mathbf{d}_{est} = \mathbf{0}$  for  $t > T_e$ , (42) can be simplified as

$$\begin{aligned} \dot{V}_s &= \frac{2}{\rho_0} \mathbf{S}^T \text{diag}(\mu_\sigma (|x_{2i}|^{\gamma-1})) \\ &\quad \times \left(\xi^{\frac{1}{k_3}} \alpha_3 \text{sig}(\mathbf{S})^{(2p_3k_3-1)/k_3} \right. \\ &\quad \left. + \xi^{\frac{1}{k_3}} \beta_3 \text{sig}(\mathbf{S})^{(2\lambda_3k_3-1)/k_3}\right)^{k_3} \\ &\leq -\sum_{i=1}^3 \left(\xi^{\frac{1}{k_3}} \alpha_3 \rho_0^{-\frac{1}{k_3}} \mu_\sigma^{\frac{1}{k_3}} (|x_{2i}|^{\gamma-1}) |S_i|^{\frac{2p_3k_3-1}{k_3} + \frac{1}{k_3}} \right. \\ &\quad \left. + \xi^{\frac{1}{k_3}} \beta_3 \rho_0^{-\frac{1}{k_3}} \mu_\sigma^{\frac{1}{k_3}} (|x_{2i}|^{\gamma-1}) |S_i|^{\frac{2\lambda_3k_3-1}{k_3} + \frac{1}{k_3}}\right)^{k_3} \\ &\leq -\left(\xi^{\frac{1}{k_3}} \mu_3 V^{p_3} + \xi^{1/k_3} \mu_4 V^{\lambda_3}\right)^{k_3} \end{aligned} \tag{43}$$

where  $\mu_3 = \alpha_3 \rho_0^{-1/k_3} \mu_\sigma^{1/k_3} (|x_{2i}|^{\gamma-1})$  and  $\mu_4 = \beta_3 \rho_0^{-1/k_3} \mu_\sigma^{1/k_3} (|x_{2i}|^{\gamma-1})$ . Applying the comparison

principle [44] and the result in Lemma 1, it is ready to conclude that  $V_s \equiv 0$  after the settling time  $T_1$  satisfying (26).

After reaching the sliding surface  $S = \mathbf{0}$ , it can be obtained from Theorem 2 that the states will be zero after the settling time  $T_s$ . Then, one can prove that the attitude Euler angles and the rotation velocity are fixed-time stable with the settling time  $T_c$  satisfying  $T_c < T_s + T_1$  regardless any initial states.

## References

- MoradiMaryamnegari, H., Khoshnood, A.M.: Robust adaptive vibration control of an underactuated flexible spacecraft. *J. Vib. Control* **25**(4), 834–850 (2019)
- Meng, T., He, W., Yang, H., Liu, J.K., You, W.: Vibration control for a flexible satellite system with output constraints. *Nonlinear Dyn.* **85**(4), 2673–2686 (2016)
- Pukdeboon, C., Jitpattanakul, A.: Anti-unwinding attitude control with fixed-time convergence for a flexible spacecraft. *Int. J. Aerosp. Eng.* **2017**, (2017)
- Tian, B., Lu, H., Zuo, Z., Wang, H.: Fixed-time stabilization of high-order integrator systems with mismatched disturbances. *Nonlinear Dyn.* **94**(4), 2889–2899 (2018)
- Chen, C.C.: A unified approach to finite-time stabilization of high-order nonlinear systems with and without an output constraint. *Int. J. Robust Nonlinear Control* **29**(2), 393–407 (2019)
- Chen, C.C., Sun, Z.Y.: Fixed-time stabilisation for a class of high-order non-linear systems. *IET Control Theory Appl.* **12**(18), 2578–2587 (2018)
- Zuo, Z.: Nonsingular fixed-time consensus tracking for second-order multi-agent networks. *Automatica* **54**, 305–309 (2015)
- Chen, C.C., Xu, S.S.D., Liang, Y.W.: Study of nonlinear integral sliding mode fault-tolerant control. *IEEE/ASME Trans. Mech.* **21**(2), 1160–1168 (2015)
- Zhao, L., Jia, Y.: Decentralized adaptive attitude synchronization control for spacecraft formation using nonsingular fast terminal sliding mode. *Nonlinear Dyn.* **78**(4), 2779–2794 (2014)
- Lee, D.: Nonlinear disturbance observer-based robust control of attitude tracking of rigid spacecraft. *Nonlinear Dyn.* **88**(2), 1317–1328 (2017)
- Cao, S., Zhao, Y.: Anti-disturbance fault-tolerant attitude control for satellites subject to multiple disturbances and actuator saturation. *Nonlinear Dyn.* **89**(4), 2657–2667 (2017)
- Chen, W.H., Yang, J., Guo, L., Li, S.: Disturbance observer-based control and related methods: an overview. *IEEE Trans. Ind. Electron.* **63**(2), 1083–1095 (2015)
- Miao, Y., Wang, F., Liu, M.: Anti-disturbance backstepping attitude control for rigid-flexible coupling spacecraft. *IEEE Access* **6**, 50729–50736 (2018)
- Liu, H., Guo, L., Zhang, Y.M.: An anti-disturbance PD control scheme for attitude control and stabilization of flexible spacecrafts. *Nonlinear Dyn.* **67**(3), 2081–2088 (2012)
- Wu, S., Chu, W., Ma, X., Radice, G., Wu, Z.: Multi-objective integrated robust H $\infty$  control for attitude tracking of a flexible spacecraft. *Acta Astron.* **151**, 80–87 (2018)
- Zhang, C., Ma, G., Sun, Y., Li, C.: Prescribed performance adaptive attitude tracking control for flexible spacecraft with active vibration suppression. *Nonlinear Dyn.* **96**(3), 1–18 (2019)
- Erdong, J., Zhaowei, S.: Passivity-based control for a flexible spacecraft in the presence of disturbances. *Int. J. Nonlinear Mech.* **45**(4), 348–356 (2010)
- Zhu, Y., Guo, L., Qiao, J., Li, W.: An enhanced anti-disturbance attitude control law for flexible spacecrafts subject to multiple disturbances. *Control Eng. Pract.* **84**, 274–283 (2019)
- Zhou, C., Zhou, D.: Robust dynamic surface sliding mode control for attitude tracking of flexible spacecraft with an extended state observer. *Proc. Inst. Mech. Eng., G. Aerosp. Eng.* **231**(3), 533–547 (2017)
- Shen, Q., Yue, C., Goh, C.H.: Velocity-free attitude reorientation of a flexible spacecraft with attitude constraints. *J. Guid. Control. Dyn.* **40**(5), 1293–1299 (2017)
- Wang, Z., Xu, M., Jia, Y., Xu, S., Tang, L.: Vibration suppression-based attitude control for flexible spacecraft. *Aerosp. Sci. Technol.* **70**, 487–496 (2017)
- Bang, H., Ha, C.-K., Kim, J.H.: Flexible spacecraft attitude maneuver by application of sliding mode control. *Acta Astron.* **57**(11), 841–850 (2005)
- Lu, K., Xia, Y.: Finite-time attitude stabilization for rigid spacecraft. *Int. J. Robust Nonlinear Control* **25**(1), 32–51 (2015)
- Jing, C., Xu, H., Niu, X., Song, X.: Adaptive nonsingular terminal sliding mode control for attitude tracking of spacecraft with actuator faults. *IEEE Access* **71**, 31485–31493 (2019)
- Lu, K., Xia, Y.: Adaptive attitude tracking control for rigid spacecraft with finite-time convergence. *Automatica* **49**(12), 3591–3599 (2013)
- Lu, K., Xia, Y., Fu, M., Yu, C.: Adaptive finite-time attitude stabilization for rigid spacecraft with actuator faults and saturation constraints. *Int. J. Robust Nonlinear Control* **26**(1), 28–46 (2016)
- Zou, A.M., Kumar, K.D.: Finite-time attitude control for rigid spacecraft subject to actuator saturation. *Nonlinear Dyn.* **96**(2), 1017–1035 (2019)
- Smaeilzadeh, S.M., Golestani, M.: A finite-time adaptive robust control for a spacecraft attitude control considering actuator fault and saturation with reduced steady-state error. *Trans. Inst. Meas. Control* **41**(4), 1002–1009 (2019)
- Huang, Y., Jia, Y.: Robust adaptive fixed-time tracking control of 6-DOF spacecraft fly-around mission for noncooperative target. *Int. J. Robust Nonlinear Control* **28**(6), 2598–2618 (2018)
- Huang, Y., Jia, Y.: Adaptive fixed-time relative position tracking and attitude synchronization control for noncooperative target spacecraft fly-around mission. *J. Franklin Inst.* **354**(18), 8461–8489 (2017)
- Gao, J., Cai, Y.: Fixed-time control for spacecraft attitude tracking based on quaternion. *Acta Astron.* **115**, 303–313 (2015)

32. Shi, X.N., Zhou, Z.G., Zhou, D.: Adaptive fault-tolerant attitude tracking control of rigid spacecraft on Lie group with fixed-time convergence. *Asian J. Control* (2019)
33. Xiao, B., Yin, S., Wu, L.: A structure simple controller for satellite attitude tracking maneuver. *IEEE Trans. Ind. Electron.* **64**(2), 1436–1446 (2016)
34. Gao, Z., Liu, X., Chen, M.: Unknown input observer based robust fault estimation for systems corrupted by partially-decoupled disturbances. *IEEE Trans. Ind. Electron.* **63**(4), 2537–2547 (2016)
35. Cong, B.L., Chen, Z., Liu, X.D.: Disturbance observer-based adaptive integral sliding mode control for rigid spacecraft attitude maneuvers. *Proc. Inst. Mech. Eng. J. Aerosp. Eng.* **227**(10), 1660–1671 (2013)
36. Li, B., Hu, Q., Ma, G.: Extended State Observer based robust attitude control of spacecraft with input saturation. *Aero. Sci. Technol.* **50**, 173–182 (2016)
37. Ran, D., Chen, X., de Ruiter, A., Xiao, B.: Adaptive extended-state observer-based fault tolerant attitude control for spacecraft with reaction wheels. *Acta Astronaut.* **145**, 501–514 (2018)
38. Ti, C., Shan, J.: Distributed adaptive fault-tolerant attitude tracking of multiple flexible spacecraft on SO (3). *Nonlinear Dyn.* **95**(3), 1827–1839 (2019)
39. Polyakov, A.: Nonlinear feedback design for fixed-time stabilization of linear control systems. *IEEE Trans. Automatic Control* **57**(8), 2106–2110 (2012)
40. Xiao, B., Hu, Q., Zhang, Y.: Adaptive sliding mode fault tolerant attitude tracking control for flexible spacecraft under actuator saturation. *IEEE Trans. Control Syst. Technol.* **20**(6), 1605–1612 (2012)
41. Levent, A.: Higher-order sliding modes, differentiation and output feedback control. *Int. J. Control* **76**(9/10), 924–941 (2003)
42. Huang, Y., Jia, Y.: Fixed-time consensus tracking control for second-order multi-agent systems with bounded input uncertainties via NFFTSM. *IET Control Theory Appl.* **11**(16), 2900–2909 (2017)
43. Bing, X., Shen, Y., Okyay, K.: Attitude stabilization control of flexible satellites with high accuracy: an estimator-based approach. *IEEE/ASME Trans. Mech.* **22**(1), 349–358 (2017)
44. Khalil, H.K.: *Nonlinear Systems*, 3rd edn. Prentice Hall, Upper Saddle River, NJ (2002)

**Publisher's Note** Springer Nature remains neutral with regard to jurisdictional claims in published maps and institutional affiliations.